

OPEN ACCESS

Spin polarized d surface resonance state of fcc Co/Cu(001)

To cite this article: K Miyamoto *et al* 2008 *New J. Phys.* **10** 125032

View the [article online](#) for updates and enhancements.

You may also like

- [Grain structure and magnetic relaxation of self-assembled Co nanowires](#)
P Schio, F J Bonilla, Y Zheng et al.
- [Study on Sn–Co Alloy Anodes for Lithium Secondary Batteries: I. Amorphous System](#)
N. Tamura, Y. Kato, A. Mikami et al.
- [Spin-polarized multi-photon photoemission and surface electronic structure of Cu\(001\)](#)
W-C Lin, A Winkelmann, C-T Chiang et al.

Spin polarized d surface resonance state of fcc Co/Cu(001)

K Miyamoto^{1,4}, K Iori¹, K Sakamoto¹, H Narita¹, A Kimura¹,
M Taniguchi^{1,2}, S Qiao², K Hasegawa², K Shimada²,
H Namatame² and S Blügel³

¹ Graduate School of Science, Hiroshima University, 1-3-1 Kagamiyama,
Higashi-Hiroshima 739-8526, Japan

² Hiroshima Synchrotron Radiation Center, Hiroshima University,
2-313 Kagamiyama, Higashi-Hiroshima 739-0046, Japan

³ Institut für Festkörperforschung, Forschungszentrum Jülich, 52425 Jülich,
Germany

E-mail: kmiyamoto@hiroshima-u.ac.jp

New Journal of Physics **10** (2008) 125032 (10pp)

Received 8 July 2008

Published 22 December 2008

Online at <http://www.njp.org/>

doi:10.1088/0031-8949/10/12/125032

Abstract. Spin- and angle-resolved photoemission spectroscopy has been applied to the study of the surface and bulk electronic structures of a face-centered cubic (fcc) Co thin film. We have experimentally resolved a negatively spin-polarized surface resonance state of fcc Co/Cu(001) at 0.4 eV below the Fermi energy. Moreover, we have found that the surface resonance state exhibits a strong spin-orbit interaction through an investigation of magnetic dichroism in the angular distribution spectrum of Co/Cu(001).

Contents

1. Introduction	2
2. Experimental	2
3. <i>Ab initio</i> calculation	3
4. Results and discussion	3
5. Conclusion	9
Acknowledgment	9
References	9

⁴ Author to whom any correspondence should be addressed.

1. Introduction

Spin-polarized electron tunneling through the surface electronic states enables us to map the spin distribution on the surface of ferro- or anti-ferromagnetic materials [1]. It also contributes to the tunneling magnetoresistance (TMR) effect [2, 3]. It is widely accepted that the magnetoresistance is mainly determined by the presence of spin polarized interfacial states between the insulating barrier and magnetic metal [4].

Spin-polarized surface electronic states of body-centered cubic (bcc) Cr(001), bcc Fe(001) and hexagonal closed packed Co(0001) have been well established and they are actually used for magnetic imaging in spin-polarized scanning tunneling microscopy (SP-STM) [2, 3]. Face-centered cubic (fcc) Co(001) is one of the most widely used ferromagnetic materials for its attractive features of epitaxial film growth and good film stability and quality. However, surface electronic states near the Fermi level (E_F) of fcc Co(001) have not been experimentally identified, although there have been several studies with spin resolved and non-spin resolved photoemission on these films [5, 6]. Recently, it has been pointed out theoretically that resonant electron tunneling should occur between fcc Co films separated by vacuum, where the electron wave number is restricted to some hot spots in the surface Brillouin zone (SBZ). Such ballistic tunneling could be caused by the formation of bonding and anti-bonding minority interface states [7]. In a realistic tunneling junction that contains an oxide barrier instead of a vacuum barrier, such surface electronic states at the ferromagnetic layer could be hybridized with the oxygen p state, a situation which might also be responsible for TMR.

Thus, the spin-polarized surface and interface states play quite important roles in atomically resolved magnetic microscopy/spectroscopy as well as in spin polarized electron tunneling through magnetic junctions. In the present paper, we have clarified the spin-polarized electronic states localized at the surface, as well as the spin-dependent bulk band structures, of fcc Co(001) thin film grown on Cu(001) by means of spin- and angle-resolved photoemission (SARPE) spectroscopy utilizing our recently developed spin polarimeter [8].

2. Experimental

A clean surface of the Cu substrate was obtained by repeated cycles of Ar-ion bombardment (1–2 keV) and annealing at 720 K in ultra high vacuum. A Co thin film was epitaxially grown on the Cu(001) single crystal using a commercial evaporator at a deposition rate of 0.1–0.2 monolayer (ML) min^{-1} in ultra-high vacuum conditions with the pressure below 3×10^{-8} Pa. The substrate was kept at room temperature during the film growth. Cleanliness of the substrate and the thin film surfaces were confirmed by Auger electron spectroscopy (AES) and reflection high-energy electron diffraction (RHEED). The film thickness was monitored by the RHEED oscillation during the Co deposition and checked later by AES. SARPE spectroscopy was performed using our homemade system equipped with a combination of a hemispherical electron analyzer and a retarding type Mott spin polarimeter [8]. The photoemission measurements were done at room temperature. We used the unpolarized He resonance line ($h\nu = 21.2$ eV) for excitation. The angular acceptance of photoelectrons was set to 2° at the pass energy of 5 eV, where the estimated total energy resolution was 110 meV. The photon incidence angle was 50° with respect to the center axis of the electron analyzer, which corresponds to the surface normal for the emission angle $\theta = 0^\circ$. The sample was magnetized along the in-plane $\langle 110 \rangle$ -direction by a coil wound around a μ -metal yoke. The

spectra were recorded by repeated scans and the direction of magnetization was switched for every sweep. Measurement time to complete one spin-resolved spectrum was as short as 20 min to avoid possible surface contamination. Although the measurement time was limited, data statistics were sufficient enough to resolve several spectral features, which are benefited from the improved efficiency of the spin detector combined with the high flux of incident photons.

3. *Ab initio* calculation

A first principles calculation was performed using density functional theory in the local density approximation (LDA). We used the full-potential linearized augmented plane-wave method. For the calculations, a cutoff of $R_{\text{MT}} K_{\text{max}} = 2.25 \times 3.8$ was used and the two-dimensional Brillouin zone was sampled with 28 special k points. We calculated a 27-layer fcc Co(001) film with an in-plane lattice constant of 2.56 Å. The interlayer distance, $d = 1.70$ Å, was deduced from a total-energy minimization with the in-plane fcc Co lattice constant being coincident with the fcc Cu(001) lattice parameter. The position of the top three layers was allowed to relax in the direction of the surface normal. Compared to the ideal interlayer distance, the first interlayer spacing contracted by 4.8%, whereas the distance between the second and the third layer expanded by 2.6%. The contraction of the third layer spacing was small (0.36%).

4. Results and discussion

Figure 1(a) represents the SARPE spectra of a 6.5 ML Co thin film on Cu (001) at various emission angles (θ) from 0° to 47° , corresponding to the $\bar{\Gamma}-\bar{X}$ line of the SBZ. Here, the open up- and the filled down-triangles indicate majority and minority spin spectra, respectively. One can see that the spectra are dominated by the minority spin intensity for all the emission angles. In contrast to the clear peak structures in the minority spin channel, the majority spin spectrum shows broad and weak features. In figure 1(b), the majority spin spectra are enlarged. At $\theta = 0^\circ$, the minority spin spectrum shows a clear double peak structure at about 0.12 (± 0.06) and 0.36 (± 0.03) eV below E_{F} , whereas the majority spin spectrum only shows a broad peak around 0.8 (± 0.1) eV. These structures are denoted as A and B for the minority spin spectrum and C for the majority spin spectrum.

Except for the structure B, these observed valence band features at $\theta = 0^\circ$ are consistent with previously reported results, where the excitation energy was similar to that used in the present case ($h\nu = 24$ eV) [9]. The improved efficiency of the present spin polarimeter combined with a high flux of the incident photons enables us to complete a measurement while the surface remains clean. One can clearly see the spin-dependent dispersion curves of fcc Co(001). With increasing θ , the structure A in the minority spin channel shifts to higher E_{B} and reaches a maximum around 37° , corresponding to the \bar{X} point. In contrast, the structure B appears only around $\theta = 0^\circ$. For the majority-spin states, the peak positions are assigned on the majority-spin spectra by the arrows in figure 1(b). Here, the thin vertical bars indicate the photoelectron signals from the Cu 3d states excited by the HeI_β satellite line; the dispersion of these features faithfully follows those appearing in the higher E_{B} region excited by HeI_α . The structure C shows an upward energy dispersion up to $\theta = 37^\circ$ and shifts back to higher E_{B} from 42° . The second majority spin state D comes in at $\theta = 12^\circ$ and shows a similar dispersion to the state C.

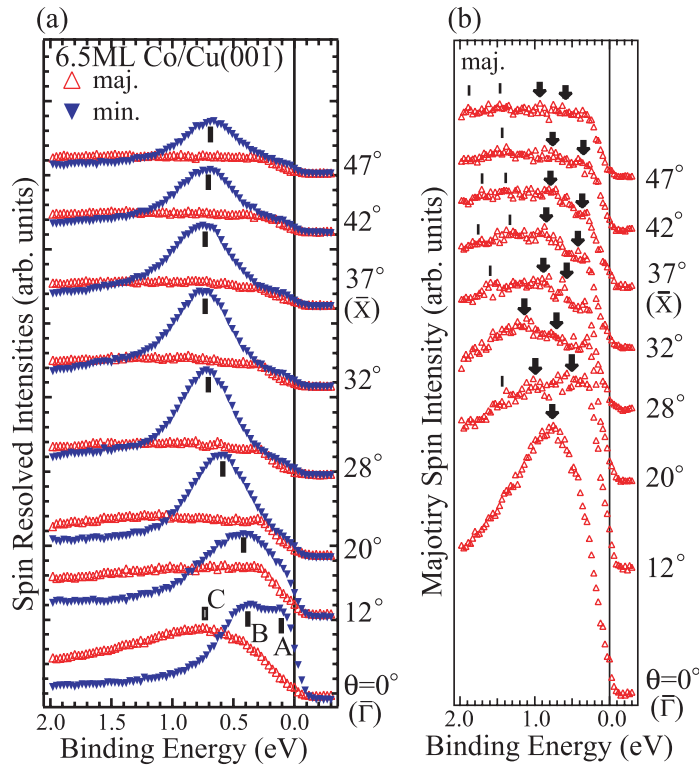


Figure 1. (a) The SARPE spectra of 6.5 ML Co/Cu(001) for emission angle (θ) from 0° to 47° . The open up-triangle (the filled down-triangle) indicates the spectra of majority (minority) spin states. The filled (open) vertical bars show the peak positions in the minority (majority) spin channel. (b) The enlarged majority spin spectra of 6.5 ML Co/Cu(001). The thin vertical bars represent the Cu 3d states excited by HeI $_{\beta}$ satellite line, whereas the arrows indicate the Co 3d states with HeI $_{\alpha}$ main line.

Next, we compare the experimental band structures of fcc Co to the results of the tight-binding calculation at the measured wave numbers ($k_{\parallel} = 0.512\sqrt{h\nu - E_B - \phi} \cdot \sin\theta$, $k_{\perp} = 0.512\sqrt{(h\nu - E_B - \phi)\cos^2\theta + V_0}$) (figure 2) assuming a free-electron parabola as the final state. Here, ϕ and V_0 are the work function (4.4 eV) and the inner-potential (15 eV) [10]. The experimental energy dispersion curves are retrieved from the intensity maxima of the observed spectra in both majority and minority spin channels. The energy positions determined in this way could sometimes deviate slightly from the realistic band structure, we believe that such minor errors do not affect the arguments used throughout the rest of this paper. For the tight-binding calculation, the transfer integrals such as ($sp\sigma$) and ($pd\sigma$) were determined not only for the first, but also for the second and third nearest-neighbor atoms so as to reproduce the result of the pseudo-potential calculation except for the exchange splitting [11]. The value of 1.5 eV was used for the exchange splitting ΔE_{ex} , which is close to the reported values of 1.4 eV by Schneider *et al* [12] and 1.55 eV by Clemens *et al* [5]. Note that the correspondence between the experimental and the calculated bands becomes worse if we use the smaller value of 1.2 eV reported by Mankey *et al* [13].

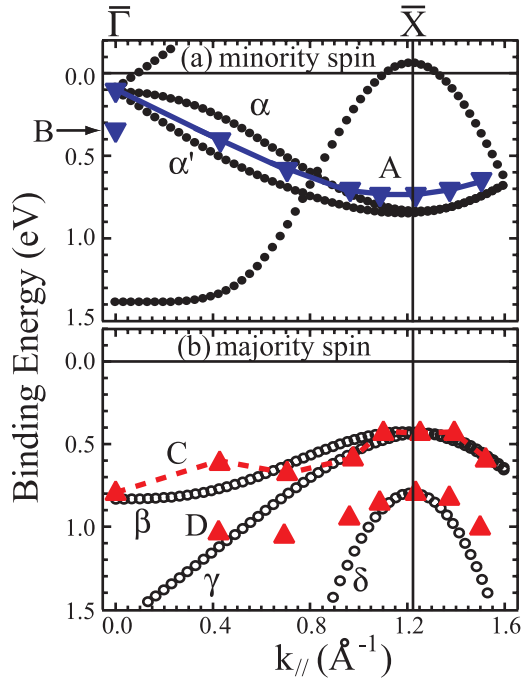


Figure 2. (a) and (b) The experimental energy band structures extracted from the SARPE spectra compared with the calculated energy dispersion curves denoted with filled (open) circles for the minority (majority) spin state projected along $\bar{\Gamma}-\bar{X}$ of the SBZ obtained by the tight-binding scheme. The down-triangle (the up-triangle) represents the peak positions of the SARPE spectra in the minority (majority) spin channel. The solid and dashed lines show the interpolated band dispersion of A and C. The calculated bands that are compared with the experimental curves are denoted as α and α' for the minority spin states, and β , γ and δ for the majority spin states.

As in figure 1, in figures 2(a) and (b), the up- and down-triangles represent the observed peak positions in the majority and minority spin channels. The open (full) circles represent the calculated band structures, and are denoted by α and α' for the minority spin, and β , γ and δ for the majority spin. The experimental band dispersions are interpolated between the data points along the solid (dashed) line for the band A (C). The experimental curve A can be assigned to the calculated band α or α' because their dispersion relations are similar to each other. Due to the limited energy and momentum resolutions, it is difficult to distinguish α or α' experimentally. In the majority spin channel, the band C corresponds to β . In contrast, no reasonable agreement is found for the second-lowest band (D). The discrepancy could be partly solved if we suppose that the data points below $k_{\parallel} \sim 0.7 \text{ \AA}^{-1}$ belong to the calculated branch γ and those above $k_{\parallel} \sim 0.8 \text{ \AA}^{-1}$ correspond to δ . In the intermediate region of $k_{\parallel} = 0.4-0.8 \text{ \AA}^{-1}$, we still find some data points that deviate from the calculated bands. This mismatch might be caused by the unresolved intensities contributed from the upper γ and the lower δ bands. Here, it should be noted that the perpendicular wave number component in the present experiment for $\theta = 0^\circ$ corresponds to the middle of the $\bar{\Gamma}-\bar{X}$ line of the fcc BZ. The observed features A and C at $\theta = 0^\circ$ are consistent with the former spin resolved ARPES experiments with tunable

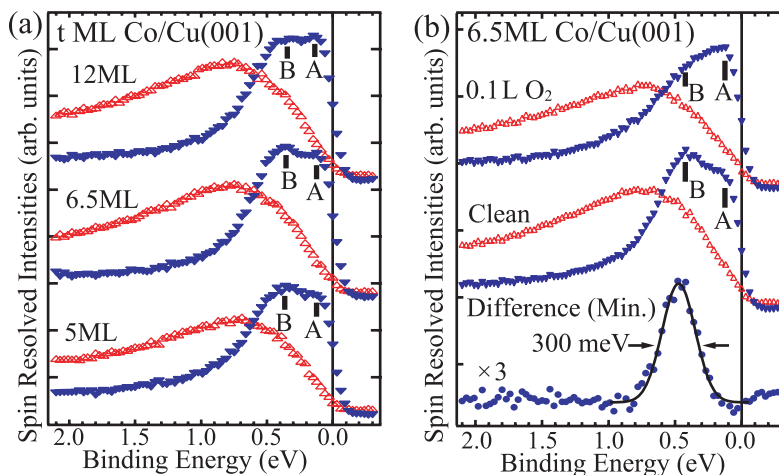


Figure 3. (a) The SARPE spectra of 5, 6.5 and 12 ML Co/Cu(001) at $\theta = 0^\circ$. (b) The SARPE spectra of clean and 0.1 L oxygen adsorbed surfaces of 6.5 ML Co film. At the bottom, the difference (dot) between clean and 0.1 L oxygen adsorbed minority spin spectra is shown as the fitted curve (solid line) by a Voigt function. Here, the open up-triangle (the filled down-triangle) represents the spectra in the majority (minority) spin channel.

photons, which disperse along the Γ -X line (normal to the [001]-direction) [5, 9, 13]. This further supports that the features A and C come from the bulk.

Thus, the observed features except for the structure B have been assigned to the bulk band. In order to check if the structure B comes from electron confinement inside the Co film, we have measured the spectra of films with various thickness. It is expected that the peak position of the quantum well state (QWS) would shift depending on the film thickness. Figure 3(a) shows the SARPE spectra for 5, 6.5 and 12 ML Co films. We find no energy shift of the peak B for all the Co film thickness. Furthermore, there is no spectral feature whose E_B is dependent on the film thickness in this energy range. Therefore, the QWS can be excluded as being responsible for B. The band structure that is relevant to QWS formation is the Δ_1 band along the Γ -X-direction. The energy gap of the Cu Δ_1 band appears in the region 2–8 eV above E_F , whereas no energy gap is formed below E_F . Based on spin-resolved inverse photoemission spectroscopy, one can expect QWS formation inside the Co film in the unoccupied state, whereas the QWS is unlikely in the occupied state [14]. This is consistent with the present result.

Next, we show the effect of oxygen adsorption on B in order to see if this feature derives from a surface state or not. Figure 3(b) shows the SARPE spectra at $\theta = 0^\circ$ of a clean Co film and one with 0.1 L of adsorbed oxygen. As can be clearly seen here, the intensity of the structure B is diminished upon oxygen adsorption, whereas the intensity of the structure A remains unchanged. Therefore, the structure B can be assigned to a surface derived electronic state. At the bottom of figure 3(b), the difference (dot) between the minority spin spectra for the clean and oxygen adsorbed surface is shown as the fitted curve (solid line) by a Voigt function. Thus, the extracted difference spectrum shows a quite symmetric feature, whose energy width and position are 300 meV (full width at half maximum (FWHM)) and 450 meV. We note that the energy width of the surface derived state is much narrower than that of bulk state (~ 600 meV). Here, one needs to consider the surface Umklapp process, which transfers the bulk state at the

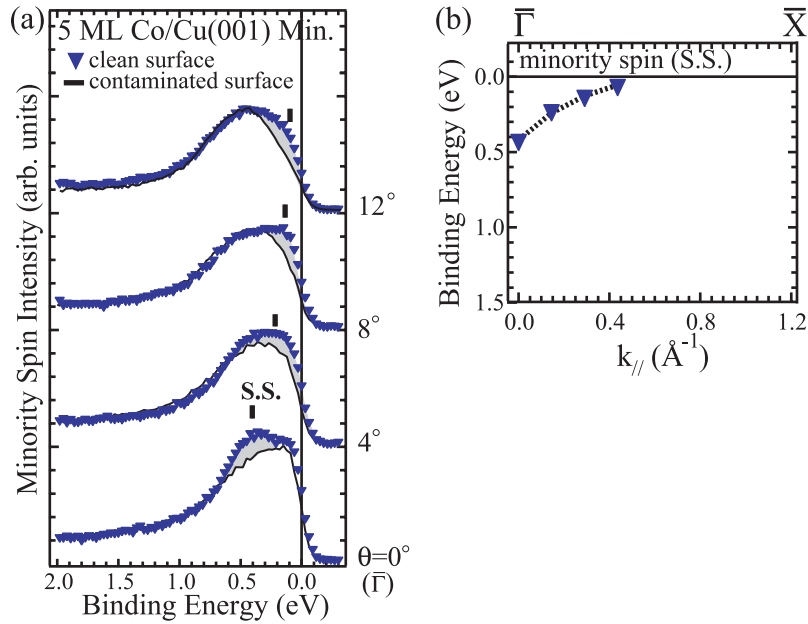


Figure 4. (a) The minority spin spectra of the clean (down-triangle) and the contaminated (thin solid line) surfaces of 5 ML Co/Cu(001) for $\theta = 0$ – 12° with 4° step. The contribution of the surface derived state is indicated by the shading. (b) The E - k dispersion curve of the surface resonance state along $\bar{\Gamma}$ - \bar{X} of SBZ.

next $\bar{\Gamma}$ of the 2nd SBZ by the reciprocal lattice vector $\mathbf{G}_{1\bar{1}0}$. In this case, one might possibly observe a similar surface-sensitive feature to the structure B. However, in that case, the energy width should be similar to, or wider than, the corresponding bulk state, which is opposite to the sharp peak observed in the present experiment. Therefore, the possibility of a bulk state derived from a surface Umklapp process can also be excluded.

Figure 4(a) exhibits the minority spin spectra (down-triangles) with a smaller angle step of 4° from $\theta = 0^\circ$ ($\bar{\Gamma}$) to 12° ($1/3\bar{\Gamma}\bar{X}$) for a clean 5 ML Co/Cu(001) surface, compared with those for the contaminated surface (thin solid line). Note that the surface derived state shifts toward E_F and it seems to cross E_F around $\theta = 12^\circ$ as clearly shown in the shaded areas of the spectra. Figure 4(b) shows the E - k relation for this minority surface state, which shows an upward dispersion and crosses E_F around $1/3\bar{\Gamma}\bar{X}$.

Figure 5 shows theoretical majority and minority spin bands obtained by an *ab initio* slab calculation for the states with even symmetry with respect to a mirror plane that is parallel to the k -vector and perpendicular to the surface of fcc Co(001). The black squares indicate the states, of which more than 50% are localized at the surface. The gray line shows the projected bulk band. The calculated surface resonance state appears around 0.55 eV below E_F at $\bar{\Gamma}$, shows an upward dispersion, and crosses E_F around $1/3\bar{\Gamma}\bar{X}$. The other surface states are found near the energy gap at 1 eV around the middle of $\bar{\Gamma}$ - \bar{X} . In contrast, we find no surface-derived states with odd symmetry along $\bar{\Gamma}$ - \bar{X} (not shown). The energy position of the calculated surface state, mainly composed of a d_{z^2} component, is close to B at $\bar{\Gamma}$ and shows an upward dispersion, crossing at $1/3\bar{\Gamma}$ - \bar{X} . These features are consistent with our experimental result. Such a minority-spin surface resonance state was not seen in the experiments previously reported with $h\nu = 45$ eV because of the s-polarized incident light, which could only probe states with odd

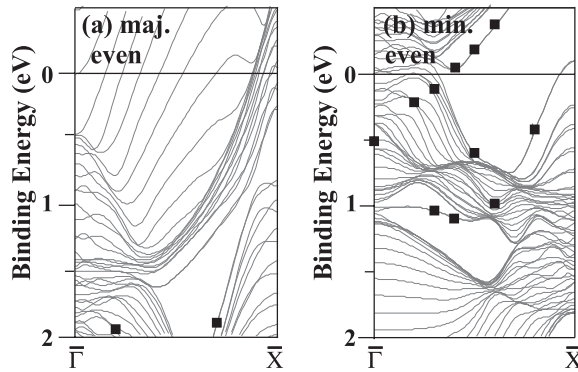


Figure 5. Surface electronic structure of the fcc Co(001) obtained by *ab initio* slab calculation. This figure is shown for majority and minority spin component with even symmetry with respect to a mirror plane that is parallel to the k -vector and perpendicular to the surface.

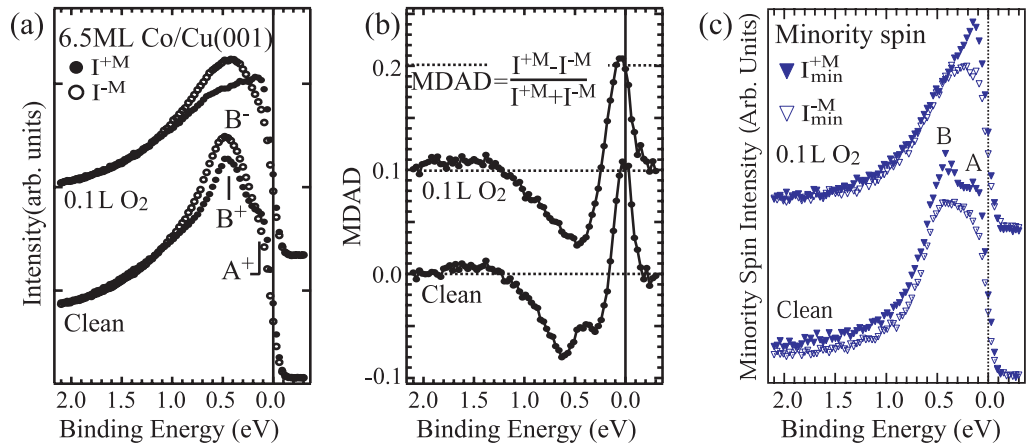


Figure 6. (a) The spin-integrated spectra of 6.5 ML Co/Cu(001) magnetized along $[110]$ (filled circle) and $[\bar{1}\bar{1}0]$ (open circle). (b) The corresponding MDAD spectra for clean and 0.1 L oxygen adsorbed Co surfaces. Here, the magnetic dichroism in angular distribution (MDAD) spectrum of the oxygen adsorbed surface is shifted by 0.1 from that of the clean surface. (c) The minority spin spectra corresponding to $+M([110])$ and $-M([\bar{1}\bar{1}0])$.

symmetry [5]. This result supports our finding of a surface resonance state with even symmetry, which is accessible only with the use of p-polarized light.

Finally, we try to elucidate the influence of spin-orbit coupling on this minority-spin surface resonance state by changing the magnetization direction, as depicted in figure 6. Here, I^{+M} and I^{-M} denote the spin integrated photoemission intensities of the clean Co thin film magnetized along $[110]$ and $[\bar{1}\bar{1}0]$. The spectrum for the plus magnetization direction contains two peaks (A^+ , B^+) at $E_B \sim 0.1$ and 0.5 eV, whereas only a single peak appears at $E_B \sim 0.5$ eV (B^-) for the minus magnetization direction. The normalized difference spectra defined as $(I^{+M} - I^{-M}) / (I^{+M} + I^{-M})$ are shown in figure 6(b). Here, these difference spectra are referred

to as MDAD. The MDAD spectrum of the clean surface shows a hump (-4%) at 0.36 eV in the negative MDAD signal and a maximum ($+10\%$) at E_F . Upon oxygen adsorption, the hump at 0.36 eV disappears and a simple dispersive structure with a minimum at 0.4 eV and maximum at E_F remains. We consider that the observed MDAD for the oxygen-covered surface originates mainly in the bulk, and is caused by the mixing between the two Co 3d bands with Δ_5 and Δ_1 symmetries under the influence of spin-orbit coupling [10]. It should be more efficient to show the dichroic effect in the spin-resolved spectra. Figure 6(c) shows the minority spin spectra with positive and negative magnetization directions denoted by filled and open triangles, respectively. The positive magnetization spectrum of the clean surface shows a sharp peak for the state B, whereas the relevant feature for the negative magnetization direction is less clear at the corresponding E_B . Upon oxygen adsorption, the sharp peak at 0.5 eV has been markedly suppressed, whereas the bulk-derived state remains unchanged. Thus, one can conclude that the minority-spin surface resonance state is also significantly influenced by the spin-orbit coupling.

5. Conclusion

In summary, we have studied the spin-dependent electronic band structures of a fcc Co thin film on Cu (001) using our new, higher efficiency, spin- and angle-resolved photoemission spectrometer. Thanks to the higher energy resolution and the reduced time needed for the measurements, we have successfully resolved the spin polarized Co 3d minority-spin surface resonance state around the $\bar{\Gamma}$ point in the SBZ. Moreover, from the MDAD spectrum, we found that the surface resonance states have a strong spin-orbit interaction. This discovery of a new surface resonance state could play an important role in SP-STM as well as in the fundamental understanding of the magnetic transport phenomena of tunneling junctions.

Acknowledgment

This work was supported by a grant-in-aid for Scientific Research from the Ministry of Education, Culture, Sports, Science and Technology (no 17340112). K Miyamoto has been supported by Grants-in-Aid from the Japanese Society for the Promotion of Science (no 175346).

References

- [1] Bode M, Getzlaff M and Wiesendanger R 1998 *Phys. Rev. Lett.* **81** 4256
- [2] Ding H F, Wulfhekel W, Henk J, Bruno P and Kirschner J 2003 *Phys. Rev. Lett.* **90** 116603
- [3] Stroscio J A, Pierce D T, Davies A, Celotta R J and Weinert M 1995 *Phys. Rev. Lett.* **75** 2960
- [4] De Teresa J M, Barthélémy A, Fert A, Contour J P, Montaigne F and Seneor P 1999 *Science* **286** 507
- [5] Clemens W, Kachel T, Rader O, Vescovo E, Blügel S, Carbone C and Eberhardt W 1992 *Solid State Commun.* **81** 739
- [6] Gao X, Koveshnikov A N, Madjoe R H, Stockbauer R L and Kurtz R L 2003 *Phys. Rev. Lett.* **90** 037603
- [7] Wunnicke O, Papanikolaou N, Zeller R, Dederichs P H, Drchal V and Kudrnovský J 2002 *Phys. Rev. B* **65** 064425
- [8] Iori K, Miyamoto K, Narita H, Sakamoto K, Kimura A, Qiao S, Shimada K, Namatame H and Taniguchi M 2006 *Rev. Sci. Instrum.* **77** 013101

- [9] Schneider C M, de Miguel J J, Bressler P, Schuster P, Miranda R and Kirschner J 1990 *J. Electron Spectrosc. Relat. Phenom.* **51** 263
- [10] Fanelsa A, Kisker E, Henk J and Feder R 1996 *Phys. Rev. B* **54** 2922
- [11] Himpsel F J, Ortega J E, Mankey G J and Willis R F 1998 *Adv. Phys.* **47** 511
- [12] Schneider C M, Schuster P, Hammond M, Ebert H, Noffke J and Kirschner J 1991 *J. Phys.: Condens. Matter* **3** 4349
- [13] Mankey G J, Willis R F and Himpsel F J 1993 *Phys. Rev. B* **48** 10284
- [14] Yu D H, Donath M, Braun J and Rangelov G 2003 *Phys. Rev. B* **68** 155415